INTERNATIONAL JOURNAL FOR NUMERICAL METHODS IN FLUIDS
*Int. J. Numer. Meth. Fluids* 2007; **54**:665–681
Published online 1 May 2007 in Wiley InterScience (www.interscience.wiley.com). DOI: 10.1002/fld.1508

# A stabilized mixed finite element method for Darcy–Stokes flow

Arif Masud*, †, ‡

*Department of Civil and Environmental Engineering, University of Illinois at Urbana-Champaign, Urbana, IL 61801, U.S.A.*

SUMMARY

This paper presents a new stabilized finite element method for the Darcy–Stokes equations also known as the Brinkman model of lubrication theory. These equations also govern the flow of incompressible viscous fluids through permeable media. The proposed method arises from a decomposition of the velocity field into coarse/resolved scales and fine/unresolved scales. Modelling of the unresolved scales corrects the lack of stability of the standard Galerkin formulation for the Darcy–Stokes equations. A significant feature of the present method is that the structure of the stabilization tensor $\boldsymbol{\tau}$ appears naturally *via* the solution of the fine-scale problem. The issue of arbitrary combinations of pressure–velocity interpolation functions is addressed, and equal-order combinations of $C^\circ$ interpolations are shown to be stable and convergent.


Received 8 January 2007; Revised 16 March 2007; Accepted 16 March 2007

KEY WORDS: multiscale finite elements; stabilized methods; Brinkman model; arbitrary pressure–velocity interpolations

## 1. INTRODUCTION

This paper presents a new stabilized mixed finite element method for the Darcy–Stokes equations. It is an extension of the stabilized mixed finite element formulation for the Darcy flow presented in Masud and Hughes [1]. A stabilized mixed discontinuous Galerkin (DG) formulation for the Darcy–Stokes equations where the pressure and velocity fields are assumed discontinuous is being developed in Masud and Hughes [2].

The stabilized method presented in Masud and Hughes [1] accommodated continuous as well as discontinuous pressure interpolations, but required the velocity interpolation to satisfy the normal continuity condition. The formulation was then extended to the DG method for the Darcy flow in Hughes *et al*. [3] where both velocity and pressure fields were considered discontinuous.

*Correspondence to: Arif Masud, Department of Civil and Environmental Engineering, University of Illinois at Urbana-Champaign, Urbana, IL 61801, U.S.A.
†E-mail: amasud@uiuc.edu
‡Associate Professor of Mechanics and Structures.

A mathematical analysis presented in Brezzi *et al*. [4] revealed that these methods may be viewed as a stable, linear combination of two unstable methods, namely, Bassi and Rebay [5] and Baumann and Oden [6]. Some recent works on stabilized methods are [1, 2, 4, 7–24].

The present method for Darcy–Stokes equations employs Hughes variational multiscale (HVM) framework wherein the velocity field is decomposed into coarse/resolved scales and fine/unresolved scales. Modelling of the unresolved scales leads to a multiscale/stabilized form of the Darcy–Stokes equations. A significant feature of the present method is that the structure of the stabilization tensor $\boldsymbol{\tau}$ appears naturally *via* the solution of the fine-scale problem. In our earlier works, we have employed similar ideas to develop multiscale/stabilized formulations for the incompressible Navier–Stokes equations [20], advection–diffusion equation [19], convective–diffusive heat transfer [7], the Darcy flow equations [1], and the Fokker–Planck equation [18].

An outline of the remainder of the paper is as follows: Section 2 presents the standard Galerkin finite element formulation. Section 3 presents the derivation of the new multiscale/stabilized formulation. Numerical simulations with one-dimensional elements employing various combinations of Lagrange polynomial interpolations, and two-dimensional linear triangles and quadrilaterals employing standard polynomial interpolations in parametric coordinates are presented in Section 4. In Section 5, we draw conclusions.

## 2. MIXED VELOCITY–PRESSURE FORMULATION

Let $\Omega \subset \mathbb{R}^{n_{\mathrm{sd}}}$ be an open-bounded region with piecewise smooth boundary $\Gamma$. The number of space dimensions, $n_{\mathrm{sd}}$, is equal to 2 or 3. Darcy–Stokes equations and conservation of mass equations are written as follows:

$$\frac{\mu}{\kappa}\mathbf{v} + \nabla p - \mu\,\Delta\mathbf{v} = \mathbf{f} \quad \text{on } \Omega \tag{1}$$

$$\operatorname{div}\mathbf{v} = \varphi \quad \text{on } \Omega \tag{2}$$

$$\mathbf{v}\cdot\mathbf{n} = \psi \quad \text{on } \Gamma \tag{3}$$

where $\mathbf{v}$ is the velocity vector, $p$ is the pressure, $\mathbf{f}$ is the body force vector, $\varphi$ is the volumetric flow rate at source or sink, $\mu>0$ is the viscosity, $\kappa>0$ is the permeability, and $\mathbf{n}$ is the unit outward normal vector to $\Gamma$. From Equations (2) and (3), the prescribed data $\varphi$ and $\psi$ are required to satisfy the constraint $\int_\Omega \varphi\,\mathrm{d}\Omega = \int_\Gamma \psi\,\mathrm{d}\Gamma$.

### 2.1. The classical weak formulation

Let

$$\mathscr{V} = H_0^1(\operatorname{div};\Omega) \stackrel{\text{def}}{=} \{\mathbf{v}\,|\,\mathbf{v}\in(L_2(\Omega))^{n_{\mathrm{sd}}},\ \operatorname{div}\mathbf{v}\in L_2(\Omega),\ \operatorname{trace}(\mathbf{v}\cdot\mathbf{n}) = \psi \text{ in } H^{1/2}(\Gamma)\} \tag{4}$$

$$\mathscr{P} = L_2(\Omega)\setminus\mathbb{R} \stackrel{\text{def}}{=} \left\{ p\,|\,p\in L_2(\Omega),\ \nabla p\in L_2(\Omega)^{n_{\mathrm{sd}}},\ \int_\Omega p\,\mathrm{d}\Omega = 0 \right\} \tag{5}$$

For further elaboration on these spaces, see Brezzi and Fortin [25].



DOI: 10.1002/fld

We assume $\kappa$, $\mu$ and $\varphi$ are given. The classical weak formulation of (1)–(3) is: find $\mathbf{v} \in \mathscr{V}$, $p \in \mathscr{P}$, such that, for all $\mathbf{w} \in \mathscr{V}$, $q \in \mathscr{P}$,

$$\left(\mathbf{w}, \frac{\mu}{\kappa}\mathbf{v}\right) - (\operatorname{div}\mathbf{w}, p) + (q, \operatorname{div}\mathbf{v}) + (\nabla\mathbf{w}, \mu\nabla\mathbf{v}) = (w, \mathbf{f}) + (q, \varphi) + (\mathbf{w}, \mu\nabla\mathbf{v})_\Gamma \tag{6}$$

where $(\cdot, \cdot)$ is the $L^2(\Omega)$ inner product. For sufficiently regular data, the weak formulation is known to possess a unique solution.

For future reference, it is convenient to rewrite (6) as follows: let $\mathscr{Y} = \mathscr{V} \times \mathscr{P}$, $\mathbf{V} = \{\mathbf{v}, p\}$ and $\mathbf{W} = \{\mathbf{w}, q\}$. Find $\mathbf{V} \in \mathscr{Y}$, such that, for all $\mathbf{W} \in \mathscr{Y}$,

$$B(\mathbf{W}, \mathbf{V}) = L(\mathbf{W}) \tag{7}$$

where

$$B(\mathbf{W}, \mathbf{V}) = \left(\mathbf{w}, \frac{\mu}{\kappa}\mathbf{v}\right) - (\operatorname{div}\mathbf{w}, p) + (q, \operatorname{div}\mathbf{v}) + (\nabla\mathbf{w}, \mu\nabla\mathbf{v}) \tag{8}$$

$$L(\mathbf{W}) = (\mathbf{w}, \mathbf{f}) + (q, \varphi) + (\mathbf{w}, \mu\nabla\mathbf{v})_\Gamma \tag{9}$$

*Remark 1*

This formulation has served as the basis of the Galerkin finite element method for the Brinkman model. A deficiency of the classical formulation is that only certain combinations of velocity and pressure interpolations are stable, such as the popular Raviart–Thomas elements [26]. In this paper, we develop a stabilized formulation that emanates from the variational multiscale ideas proposed by Hughes [27]. The new form is inherently more stable, and accommodates a greater variety of stable interpolations, such as arbitrary combinations of continuous interpolations, which are known to be unstable in the classical formulation.

## 3. HUGHES VARIATIONAL MULTISCALE METHOD

### *3.1. Multiscale decomposition*

We consider the bounded domain $\Omega$ discretized into $n_{el}$ non-overlapping regions $\Omega^e$ (element domains) with boundaries $\Gamma^e$, $e = 1, 2, \ldots, n_{el}$, and we denote the union of element interiors and element boundaries by $\Omega'$ and $\Gamma'$, respectively:

$$\Omega' = \bigcup_{e=1}^{n_{el}} (\text{int})\Omega^e \quad \text{(element interiors)} \tag{10}$$

$$\Gamma' = \bigcup_{e=1}^{n_{el}} \Gamma^e \quad \text{(element boundaries)} \tag{11}$$

We assume an overlapping sum decomposition of the velocity field into coarse scales or resolvable scales and fine scales or the subgrid scales. Fine scales can be viewed as components associated with the regions of high velocity gradients:

$$\mathbf{v}(\mathbf{x}) = \underbrace{\bar{\mathbf{v}}(\mathbf{x})}_{\text{coarse scale}} + \underbrace{\mathbf{v}'(\mathbf{x})}_{\text{fine scale}} \tag{12}$$



DOI: 10.1002/fld

Likewise, we assume an overlapping sum decomposition of the weighting function into coarse and fine-scale components indicated as $\bar{\mathbf{w}}$ and $\mathbf{w}'$, respectively:

$$\mathbf{w}(\mathbf{x}) = \underbrace{\bar{\mathbf{w}}(\mathbf{x})}_{\text{coarse scale}} + \underbrace{\mathbf{w}'(\mathbf{x})}_{\text{fine scale}} \tag{13}$$

We further make an assumption that the subgrid scales although non-zero within the elements, vanish identically over the element boundaries, i.e. $\mathbf{v}'(\mathbf{x}) = \mathbf{w}' = \mathbf{0}$ on $\Gamma$.

We now introduce the appropriate spaces of functions for the coarse and fine-scale fields and specify a direct sum decomposition on these spaces, i.e. $\mathscr{V} = \bar{\mathscr{V}} \oplus \mathscr{V}'$, where $\bar{\mathscr{V}}$ is the space of trial solutions and weighting functions for the coarse scale velocity field and is identified with the standard finite element space. On the other hand, various characterizations of $\mathscr{V}'$ are possible, subject to the restriction imposed by the stability of the formulation that requires $\bar{\mathscr{V}}$ and $\mathscr{V}'$ to be linearly independent. Consequently, in the discrete case $\mathscr{V}'$ can contain various finite dimensional approximations, e.g. bubble functions or $p$-refinements.

*Remark 2*

The pressure field can also be decomposed into coarse and fine scales. However, without loss of generality, we assume that the fine-scale pressure field is zero. This assumption helps in eliminating the terms that would otherwise emanate from the fine-scale part of the weak form of the continuity equation.

### *3.2. The multiscale variational problem*

We now substitute trial solutions (12) and weighting functions (13) in standard variational form (6), and this becomes the point of departure from the conventional Galerkin formulations. With suitable assumptions on the fine-scale field, and employing the linearity of the weighting function, we can split the problem into coarse and fine-scale parts.

The coarse-scale sub-problem $\bar{\mathscr{W}}$ and the fine-scale problem $\mathscr{W}'$ can be written as follows:

*The coarse-scale problem*:

$$\left(\bar{\mathbf{w}}, \frac{\mu}{\kappa}(\bar{\mathbf{v}} + \mathbf{v}')\right) + (\nabla\bar{\mathbf{w}}, \mu\nabla(\bar{\mathbf{v}} + \mathbf{v}')) - (\operatorname{div}\bar{\mathbf{w}}, p) + (q, \operatorname{div}(\bar{\mathbf{v}} + \mathbf{v}'))$$
$$= (\bar{\mathbf{w}}, \mathbf{f}) + (q, \varphi) + (\bar{\mathbf{w}}, \mu\nabla\mathbf{v})_\Gamma \tag{14}$$

*The fine-scale problem*:

$$\left(\mathbf{w}', \frac{\mu}{\kappa}(\bar{\mathbf{v}} + \mathbf{v}')\right) + (\nabla\mathbf{w}', \mu\nabla(\bar{\mathbf{v}} + \mathbf{v}')) - (\operatorname{div}\mathbf{w}', p) = (\mathbf{w}', \mathbf{f}) \tag{15}$$

The key idea at this point is to solve fine-scale problem (15), defined over the sum of element interiors, to obtain the fine-scale solution $\mathbf{v}'$. This solution is then substituted in the coarse-scale problem given by (14), thereby eliminating the explicit appearance of the fine scales $\mathbf{v}'$ while still modelling their effects.

### *3.3. Solution of the fine-scale problem ($\mathscr{W}'$)*

Let us consider the fine-scale part of the weak form $\mathscr{W}'$, which, because of the assumption on the fine-scale space, is defined over $\Omega'$. Employing linearity of the solution slot in Equation (15), and



DOI: 10.1002/fld

rearranging terms, we get

$$\left(\mathbf{w}', \frac{\mu}{\kappa}\mathbf{v}'\right) + (\nabla\mathbf{w}', \mu\nabla\mathbf{v}') = (\mathbf{w}', \mathbf{f}) - \left(\mathbf{w}', \frac{\mu}{\kappa}\bar{\mathbf{v}}\right) - (\mathbf{w}', \nabla p) - (\nabla\mathbf{w}', \mu\nabla\bar{\mathbf{v}}) \tag{16}$$

$$= \left(\mathbf{w}', \left(\mathbf{f} - \frac{\mu}{\kappa}\bar{\mathbf{v}} - \nabla p + \mu\Delta\bar{\mathbf{v}}\right)\right) \tag{17}$$

$$= (\mathbf{w}', \bar{\mathbf{r}}) \tag{18}$$

where $\bar{\mathbf{r}} = \mathbf{f} - (\mu/\kappa)\bar{\mathbf{v}} - \nabla p + \mu\Delta\bar{\mathbf{v}}$. We have applied integration by parts, and assumption that $\mathbf{w}' = 0$ on $\Gamma'$ to the fourth integral on the right-hand side of (16) to arrive at (17).

Our objective at this point is to solve (18) either analytically or numerically to extract the fine-scale solution $\mathbf{v}'$ that can then be substituted in the coarse-scale problem $\bar{\mathscr{W}}$. This would eliminate the explicit dependence of (14) on $\mathbf{v}'$, while the ensuing terms will model the effect of $\mathbf{v}'$. Hughes [27] has proposed a Green's function approach for the solution of the fine-scale problem. Brezzi and co-workers [8–10] present a way to solve the fine-scale problem *via* residual-free bubbles, while Franca and Nesliturk [17] propose a two-level finite element approach to perform this task. An equivalence between the three approaches is presented in [11].

*Remark 3*
The right-hand side of (18) is a function of the residual of the Euler–Lagrange equations for the coarse scales over the sum of element interiors. This is an important ingredient of the present multiscale method and ensures that the resultant formulation yields a consistent method.

*Remark 4*
The solution of the fine-scale problem can also be accomplished in the DG framework. A full DG formulation of the Darcy–Stokes equations is presented in Masud and Hughes [2].

In order to keep the presentation simple, and to extract the structure of the stability tensor $\boldsymbol{\tau}$, we employ bubble functions. To crystallize ideas, and without loss of generality, we assume that the fine scales $\mathbf{v}'$ and $\mathbf{w}'$ are represented *via* bubbles over $\Omega'$, i.e.

$$\mathbf{v}'|_{\Omega^e} = b^e(\boldsymbol{\xi})\boldsymbol{\beta} \rightarrow \mathbf{v}'_i|_{\Omega^e} = b^e(\boldsymbol{\xi})\boldsymbol{\beta}_i \quad \text{on } \Omega^e \tag{19}$$

$$\mathbf{w}'|_{\Omega^e} = b^e(\boldsymbol{\xi})\boldsymbol{\gamma} \rightarrow \mathbf{w}'_i|_{\Omega^e} = b^e(\boldsymbol{\xi})\boldsymbol{\gamma}_i \quad \text{on } \Omega^e \tag{20}$$

where $b^e$ represents the bubble shape functions over element domains, $i = 1 \ldots n_{\text{sd}}$ and $\boldsymbol{\beta}$ and $\boldsymbol{\gamma}$ represent the coefficients for the fine-scale trial solutions and weighting functions, respectively.

Substituting (19) and (20) in (18) and taking the vectors of constant coefficients out of the integral expression, we get

$$\boldsymbol{\gamma}^{\mathrm{T}}\left(\int_{\Omega^e} b^e\frac{\mu}{\kappa}b^e\,\mathrm{d}\Omega\,\mathbf{I} + \int_{\Omega^e}\mu|\nabla b^e|^2\,\mathrm{d}\Omega\,\mathbf{I} + \int_{\Omega^e}\mu\nabla b^e\otimes\nabla b^e\,\mathrm{d}\Omega\right)\boldsymbol{\beta} = \boldsymbol{\gamma}^{\mathrm{T}}(b^e, \bar{\mathbf{r}}) \tag{21}$$

Since $\boldsymbol{\gamma}$ is arbitrary, consequently we have

$$\boldsymbol{\beta} = \mathbf{K}^{-1}\mathbf{R} \tag{22}$$



DOI: 10.1002/fld

where $\mathbf{K}$ and $\mathbf{R}$ are defined as follows:

$$\mathbf{K} = \int_{\Omega^e} b^e \frac{\mu}{\kappa} b^e \, \mathrm{d}\Omega \, \mathbf{I} + \mu \int_{\Omega^e} |\nabla b^e|^2 \, \mathrm{d}\Omega \, \mathbf{I} + \mu \int_{\Omega^e} \nabla b^e \otimes \nabla b^e \, \mathrm{d}\Omega \tag{23}$$

$$\mathbf{R} = \int_{\Omega^e} b^e \bar{\mathbf{r}} \, \mathrm{d}\Omega \tag{24}$$

where $\mathbf{I}$ is a $n_{\mathrm{sd}} \times n_{\mathrm{sd}}$ identity matrix, $\nabla b$ is a $n_{\mathrm{sd}} \times 1$ vector of gradient of bubble functions. We now reconstruct the fine-scale field over the sum of element domains $\Omega'$ *via* recourse to (19):

$$\begin{aligned} \mathbf{v}'(\mathbf{x}) &= b^e(\boldsymbol{\xi})\boldsymbol{\beta} \\ &= b^e(\boldsymbol{\xi})\mathbf{K}^{-1}\mathbf{R} \end{aligned} \tag{25}$$

### *3.4. Solution of the coarse-scale problem ($\bar{\mathscr{W}}$)*

Let us now consider the coarse-scale part of the weak form $\bar{\mathscr{W}}$. Exploiting linearity of the solution slot, Equation (14) can be written as

$$\begin{aligned} &\left(\bar{\mathbf{w}}, \frac{\mu}{\kappa}\bar{\mathbf{v}}\right) + \left(\bar{\mathbf{w}}, \frac{\mu}{\kappa}\mathbf{v}'\right) + (\nabla\bar{\mathbf{w}}, \mu\nabla\bar{\mathbf{v}}) + (\nabla\bar{\mathbf{w}}, \mu\nabla\mathbf{v}') - (\operatorname{div}\bar{\mathbf{w}}, p) + (q, \operatorname{div}\bar{\mathbf{v}}) + (q, \operatorname{div}\mathbf{v}') \\ &\quad = (\bar{\mathbf{w}}, \mathbf{f}) + (q, \varphi) + (\mathbf{w}, \mu\nabla\mathbf{v})_\Gamma \end{aligned} \tag{26}$$

Consider the fourth term on the left-hand side of (26) and apply integration by parts

$$(\nabla\bar{\mathbf{w}}, \mu\nabla\mathbf{v}')_\Omega = (\nabla\bar{\mathbf{w}}, \mu\mathbf{v}')|_\Gamma - (\Delta\bar{\mathbf{w}}, \mu\mathbf{v}')_\Omega \tag{27}$$

Accordingly, the coarse-scale problem (26) can be written as

$$\begin{aligned} &\left(\bar{\mathbf{w}}, \frac{\mu}{\kappa}\bar{\mathbf{v}}\right) + (\nabla\bar{\mathbf{w}}, \mu\nabla\bar{\mathbf{v}}) - (\operatorname{div}\bar{\mathbf{w}}, p) + (q, \operatorname{div}\bar{\mathbf{v}}) + \left(\bar{\mathbf{w}}, \frac{\mu}{\kappa}\mathbf{v}'\right) - (\Delta\bar{\mathbf{w}}, \mu\mathbf{v}') - (\nabla q, \mathbf{v}') \\ &\quad = (\bar{\mathbf{w}}, \mathbf{f}) + (q, \varphi) + (\mathbf{w}, \mu\nabla\mathbf{v})_\Gamma \end{aligned} \tag{28}$$

In Equation (28), $\mathbf{v}'$ appears in fifth, sixth and seventh terms on the left-hand side. Substituting $\mathbf{v}'$ from (25), and with the assumption that the projection of the residual $\bar{\mathbf{r}}$ is constant over element interiors, we get the following HVM-stabilized form of the Darcy–Stokes equation. Since the resulting equation is expressed entirely in terms of the coarse scales, for the sake of simplicity, the superposed bars are dropped:

$$\begin{aligned} &\left(\mathbf{w}, \frac{\mu}{\kappa}\mathbf{v}\right) + (\nabla\mathbf{w}, \mu\nabla\mathbf{v}) - (\operatorname{div}\mathbf{w}, p) + (q, \operatorname{div}\mathbf{v}) \\ &\qquad + \left(-\frac{\mu}{\kappa}\mathbf{w} + \nabla q + \mu\,\Delta\mathbf{w}, \boldsymbol{\tau}\left(\frac{\mu}{\kappa}\mathbf{v} + \nabla p - \mu\,\Delta\mathbf{v} - \mathbf{f}\right)\right) \\ &\quad = (\mathbf{w}, \mathbf{f}) + (q, \varphi) + (\mathbf{w}, \mu\nabla\mathbf{v})_\Gamma \end{aligned} \tag{29}$$



DOI: 10.1002/fld

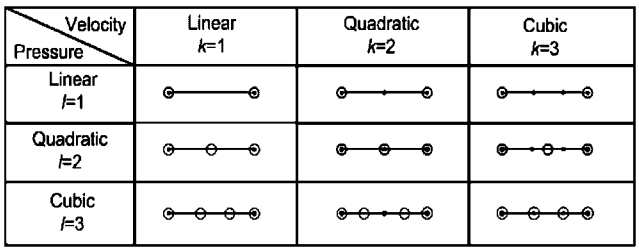


Figure 1. Continuous pressure–velocity elements in one dimension.

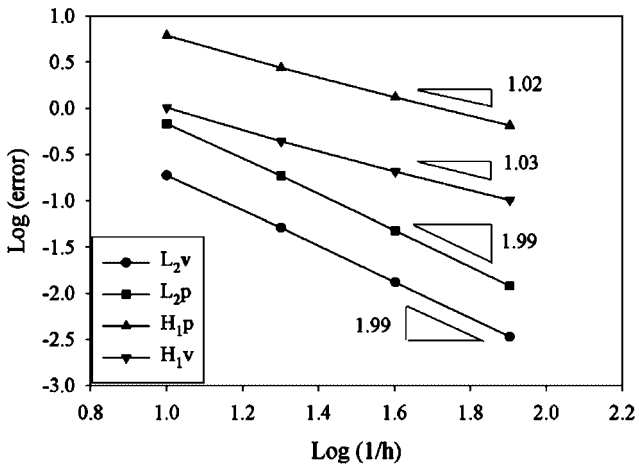


Figure 2. Convergence rates for linear equal-order one-dimensional elements.

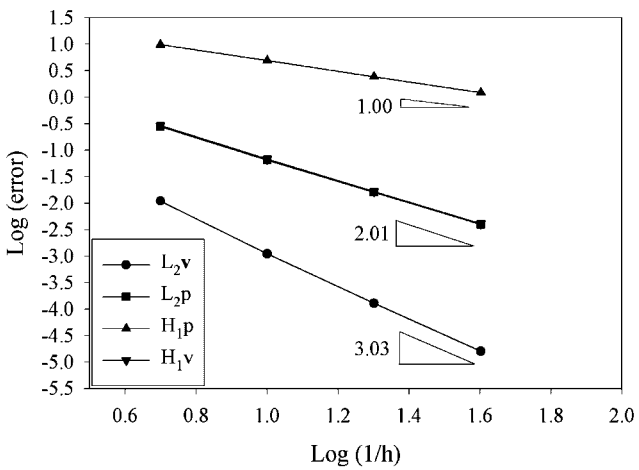


Figure 3. Convergence rates for quadratic equal-order one-dimensional elements.



DOI: 10.1002/fld

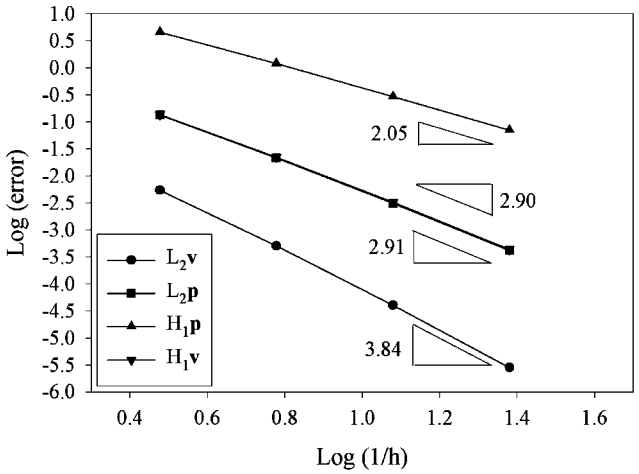


Figure 4. Convergence rates for cubic equal-order one-dimensional elements.

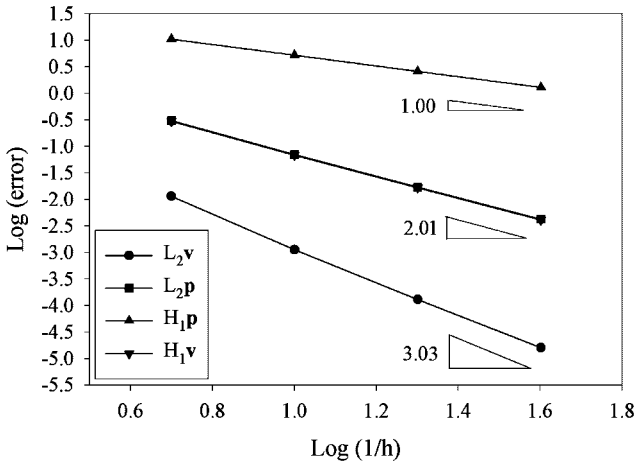


Figure 5. Convergence rates for quadratic-velocity linear-pressure one-dimensional elements.

where $\tau$ is defined as

$$\tau = \left( b^e \int_{\Omega^e} b^e \, \mathrm{d}\Omega \right) \left[ \int_{\Omega^e} b^e \frac{\mu}{\kappa} b^e \, \mathrm{d}\Omega \, \mathbf{I} + \mu \int_{\Omega^e} |\nabla b^e|^2 \, \mathrm{d}\Omega \, \mathbf{I} + \mu \int_{\Omega^e} \nabla b^e \otimes \nabla b^e \, \mathrm{d}\Omega \right]^{-1} \tag{30}$$

It is important to note that the fifth term on the left-hand side has appeared because of the assumption of existence of fine scales in the problem. This term is in fact modelling the numerical subgrid scales in the problem. Since the method is residual based, therefore the resulting formulation is consistent and accommodates the exact solution. Another important feature of this formulation



DOI: 10.1002/fld

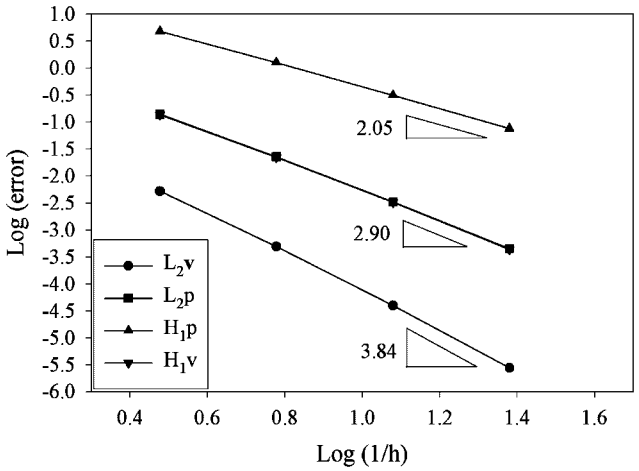


Figure 6. Convergence rates for cubic-velocity quadratic-pressure one-dimensional elements.

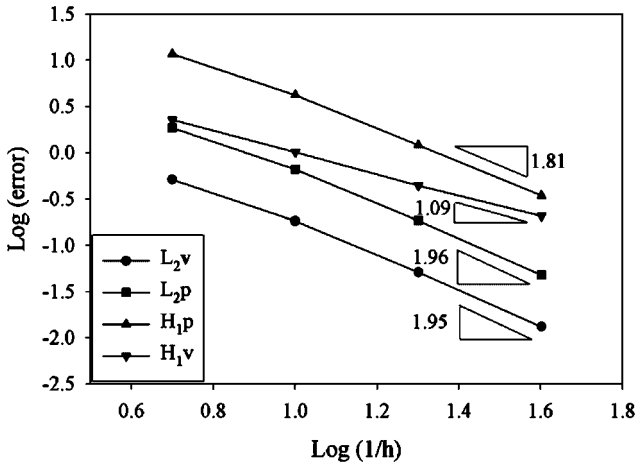


Figure 7. Convergence rates for linear-velocity quadratic-pressure one-dimensional elements.

is that the structure of the stabilization tensor $\boldsymbol{\tau}$ has appeared naturally *via* the solution of the fine-scale part of the problem.

*Remark 5*
It is important to note that the bubble functions only reside in the definition of the stability tensor $\boldsymbol{\tau}$. Consequently, the choice of the bubble functions only affects the value of the stability tensor.

*Remark 6*
From the definition of $\boldsymbol{\tau}$ given in (30), in the Darcy limit $\boldsymbol{\tau}$ is $O(\kappa(\mathbf{x})/\mu(\mathbf{x}))$ while in the Stokes limit $\boldsymbol{\tau}$ is $O(h^2/\mu(\mathbf{x}))$. To keep the definition simple in the numerical calculations, we use the



DOI: 10.1002/fld

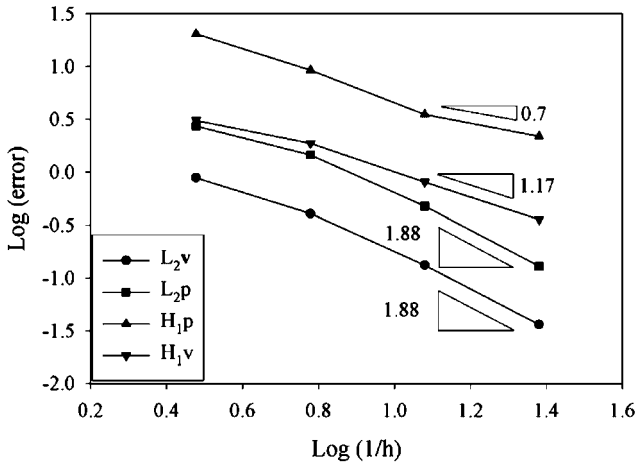


Figure 8. Convergence rates for linear-velocity cubic-pressure one-dimensional elements.

following definition of $\boldsymbol{\tau}$ [1] in the calculations presented in Section 4:

$$\boldsymbol{\tau} = \tfrac{1}{2}\tau^e \boldsymbol{\delta}$$

where

$$\tau^e = \min_{\mathbf{x}\in\Omega^e} \left\{ \frac{\beta h^2}{\mu(\mathbf{x})}, \frac{\kappa(\mathbf{x})}{\mu(\mathbf{x})} \right\} \tag{31}$$

where $\beta$ is a non-dimensional constant which depends on the element type [28, 29]. In our numerical calculations, the element mesh parameter '$h$' is taken to be the edge length of the elements for quadrilaterals, and the short-edge length for triangles. A discussion on the selection of element characteristic length scale $h$ is presented in Harari and Hughes [30] and in Tezduyar [23].

### *3.5. The multiscale/stabilized weak formulation*

The HVM stabilized weak formulation is: find $\mathbf{V} \in \mathscr{Y}$, such that, for all $\mathbf{W} \in \mathscr{Y}$,

$$B_{\text{stab}}(\mathbf{W}, \mathbf{V}) = L_{\text{stab}}(\mathbf{W}) \tag{32}$$

where

$$B_{\text{stab}}(\mathbf{W}, \mathbf{V}) = B(\mathbf{W}, \mathbf{V}) + \frac{1}{2}\left(\left(-\frac{\mu}{\kappa}\mathbf{w} + \nabla q + \mu\Delta\mathbf{w}\right), \tau^e\left(\frac{\mu}{\kappa}\mathbf{v} + \nabla p - \mu\Delta\mathbf{v}\right)\right) \tag{33}$$

$$L_{\text{stab}}(\mathbf{W}) = L(\mathbf{W}) + \frac{1}{2}\left(\left(-\frac{\mu}{\kappa}\mathbf{w} + \nabla q + \mu\Delta\mathbf{w}\right), \tau^e\mathbf{f}\right) \tag{34}$$

and $B(\mathbf{W}, \mathbf{V})$ and $L(\mathbf{W})$ are given by (8) and (9), respectively.



DOI: 10.1002/fld

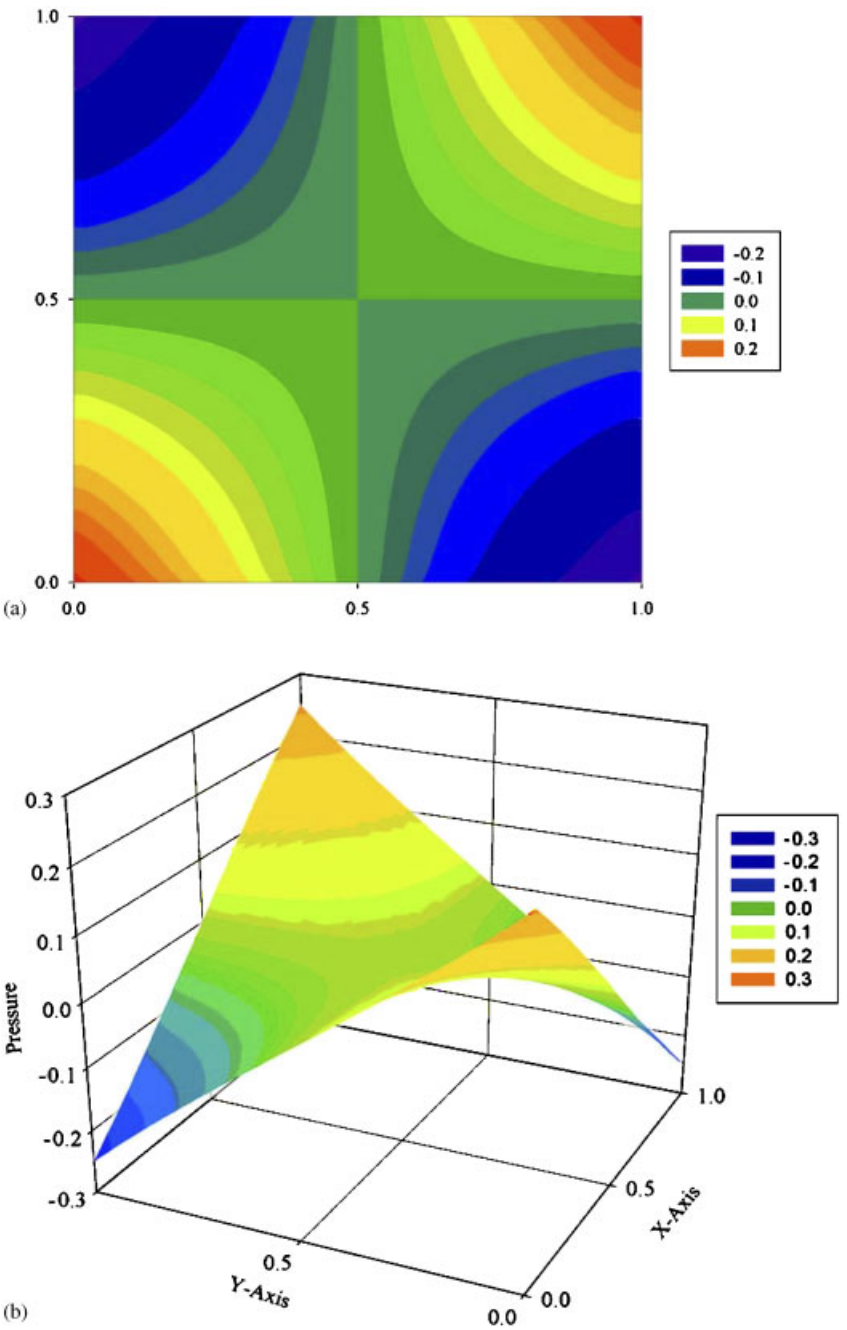


Figure 9. (a) Contour plot of the exact pressure field and (b) elevation plot of the exact pressure field.



DOI: 10.1002/fld

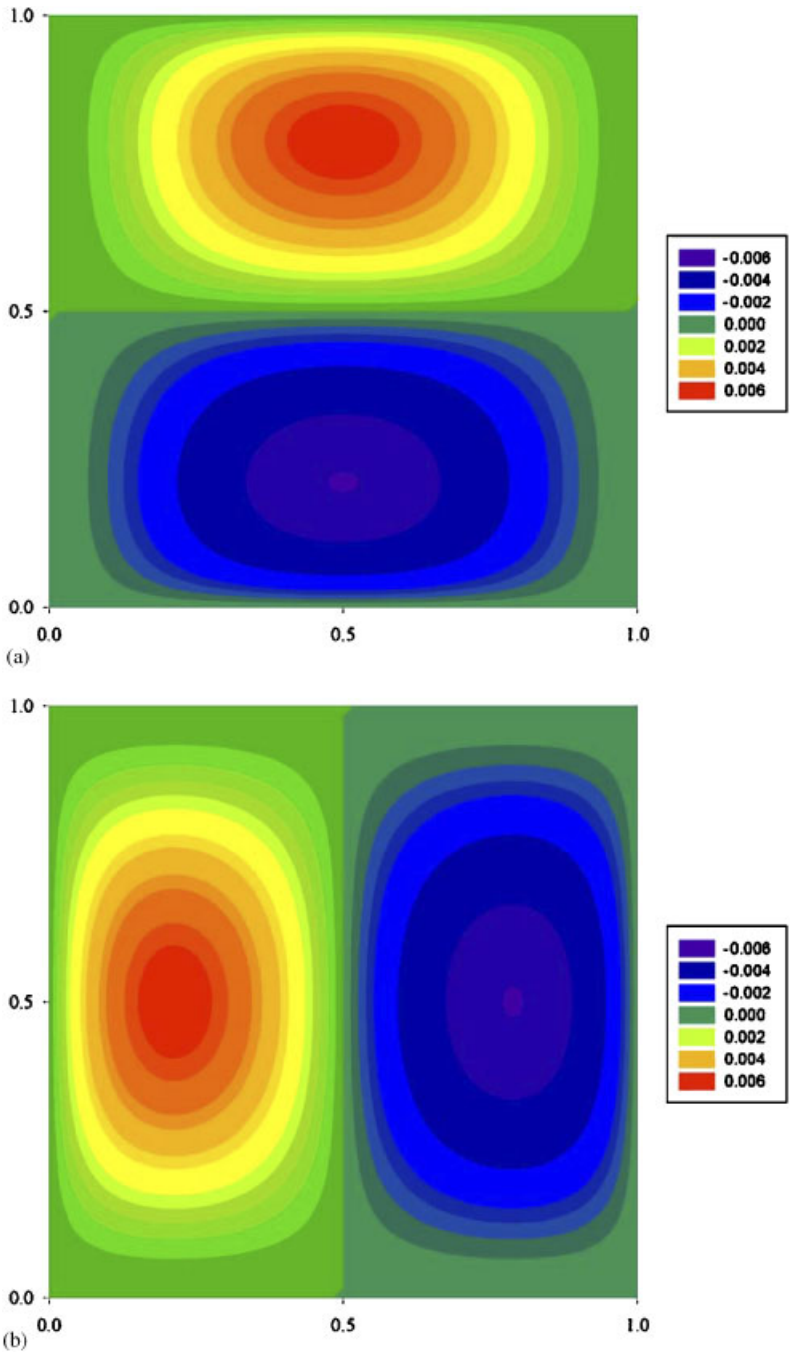


Figure 10. (a) Contour plot: (a) of the $v_x$ component of the exact velocity field and (b) of the $v_y$ component of the exact velocity field.



DOI: 10.1002/fld

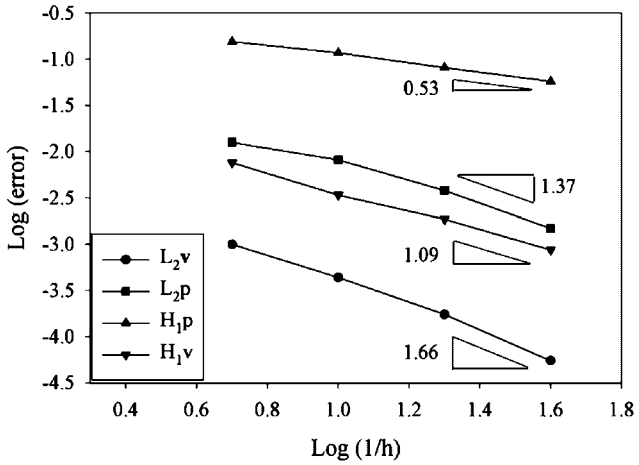


Figure 11. Convergence rates for equal-order bilinear quadrilaterals.

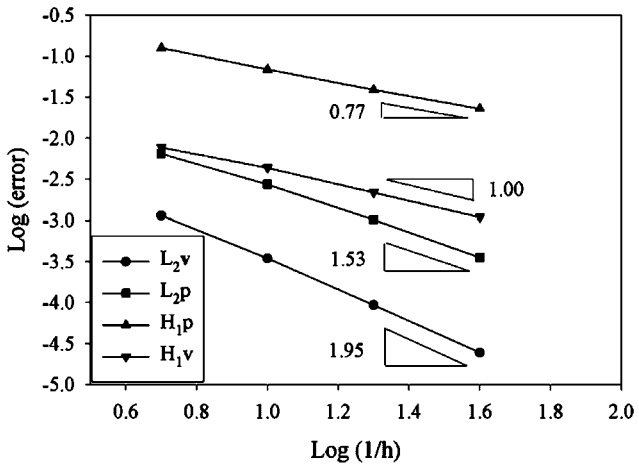


Figure 12. Convergence rates for equal-order linear triangles.

## 4. NUMERICAL EXAMPLES

This section presents numerical convergence study with one- and two-dimensional elements. In all cases, standard Lagrange interpolation functions together with sufficiently high integration rules are employed [31, Chapter 3].

### *4.1. Convergence study for one-dimensional elements*

The domain under consideration is $\Omega = [0, 1]$. The exact pressure solution is given by

$$p = \sin 2\pi x \tag{35}$$



DOI: 10.1002/fld

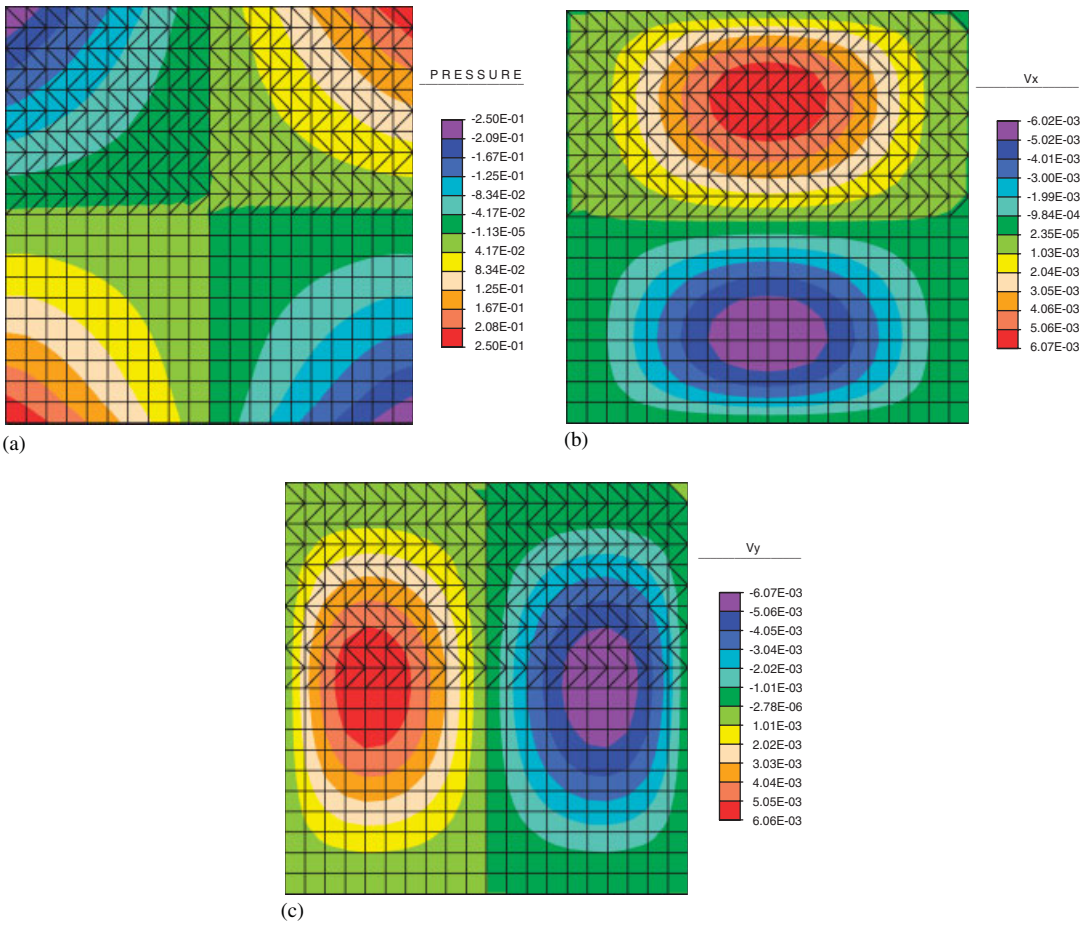


Figure 13. (a) Contour plot of the pressure field for bilinear equal-order quadrilaterals. Two-hundred 4-node and 400 3-node element mesh. Contour plot (b) of the $v_x$ component and (c) of the $v_y$ component of the velocity field for bilinear equal-order quadrilaterals. Two-hundred 4-node and 400 3-node element mesh.

The velocity field is computed from Darcy–Stokes equation in which $\kappa/\mu = 1$, $\varphi$ is calculated by taking the derivative of the velocity field, and $\psi$ is calculated by taking its normal component. In specifying the boundary-value problem, $\varphi$ is prescribed over $\Omega$ while $\psi$ is prescribed at the boundary. Uniform meshes were employed in obtaining the results presented in this section.

Figure 1 shows the continuous velocity–pressure elements studied. Dots correspond to the velocity nodes and circles correspond to the pressure nodes. Numerically attained convergence rates for the various combinations of velocity and pressure interpolations are presented in Figures 2–8.



DOI: 10.1002/fld

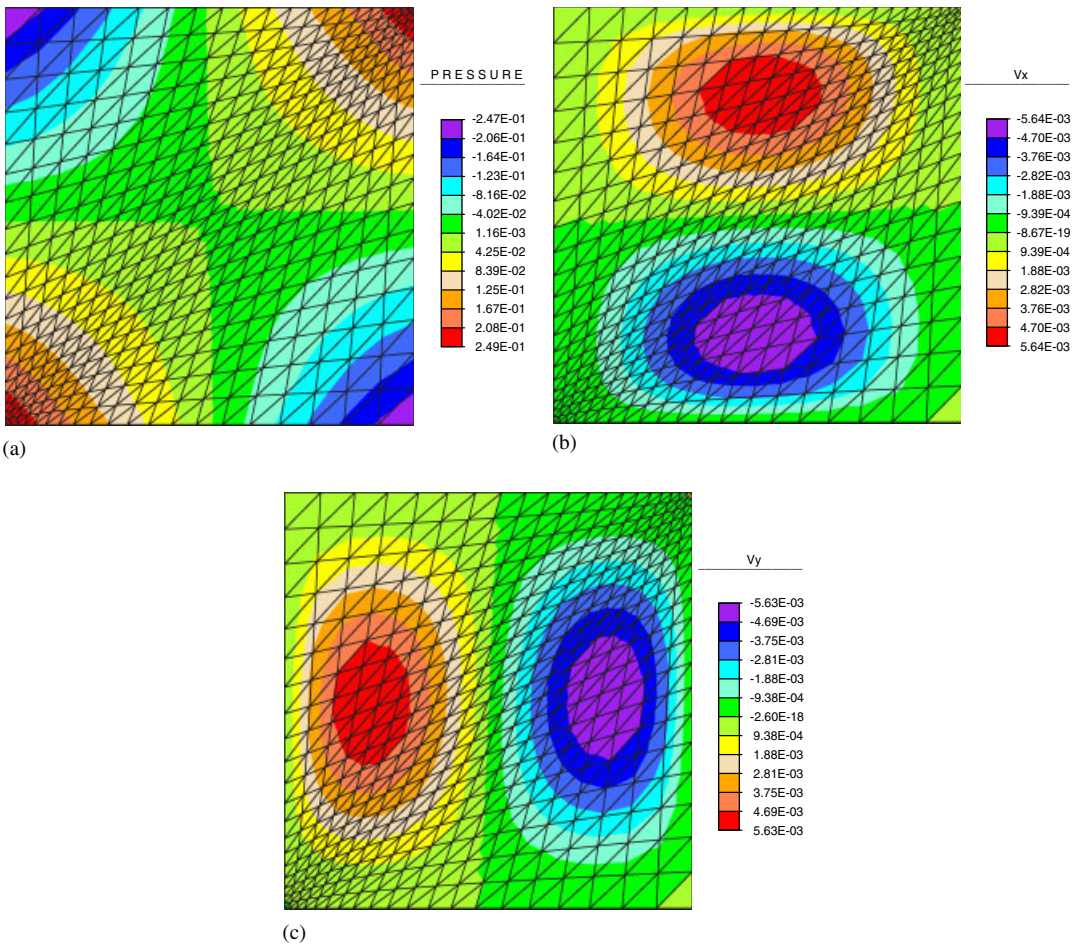


Figure 14. (a) Contour plot of the pressure field for bilinear equal-order quadrilaterals. Contour plot (b) of the $v_x$ component and (c) of the $v_y$ component of the velocity field.

### *4.2. Convergence study for two-dimensional linear elements*

The domain under consideration is $\Omega = [0, 1] \times [0, 1]$. The exact solution to the problem is given by

$$v_x(x, y) = -x^2(x-1)^2 y(y-1)(2y-1) \tag{36}$$

$$v_y(x, y) = -v_x(y, x) \tag{37}$$

$$p(x, y) = (x - \tfrac{1}{2})(y - \tfrac{1}{2}) \tag{38}$$

Substituting the velocity and pressure field in (1) yields the body force vector that is then numerically integrated over the domain. In specifying the boundary-value problem, $\mathbf{v} = \mathbf{0}$ is prescribed nodally at the boundary. A contour plot and elevation plot of the exact pressure are shown in



DOI: 10.1002/fld

Figure 9(a) and (b). Figure 10(a) and (b) presents contours of the components of the exact velocity field. The element mesh parameter, $h$, is taken to be the edge length of the elements for quadrilaterals, and the short-edge length for triangles. Convergence rates for equal-order bilinear quadrilateral and linear triangles are presented in Figures 11 and 12. The results are consistent with the corresponding one-dimensional cases.

Computed pressure and velocity field for the composite mesh composed of linear triangles and bilinear quadrilaterals are shown in Figure 13(a)–(c). Likewise, contour plots for the computed pressure and velocity field for the distorted mesh of linear triangles are shown in Figure 14(a)–(c). In both cases, stable velocity and pressure fields are obtained.

## 5. CONCLUSIONS

We have presented a new stabilized finite element method for the Darcy–Stokes equations. Underlying idea is a decomposition of the velocity field into coarse/resolved scales and fine/unresolved scales. Modelling of the unresolved scales yields the stabilized form. An important feature of the method is that the structure of the stabilization tensor $\boldsymbol{\tau}$ appears naturally *via* the solution of the fine-scale problem. Numerical tests show stable and convergent behaviour for various combinations of velocity–pressure interpolations. Preliminary results on two-dimensional linear elements also show similar stable and convergent behaviour.

ACKNOWLEDGEMENT

The author wishes to thank Professor T. J. R. Hughes for many helpful discussions.

REFERENCES

1. Masud A, Hughes TJR. A stabilized mixed finite element method for Darcy flow. *Computer Methods in Applied Mechanics and Engineering* 2002; **191**(39–40):4341–4370.
2. Masud A, Hughes TJR. Stabilized mixed discontinuous Galerkin methods for Darcy–Stokes flow, in preparation.
3. Hughes TJR, Masud A, Wan J. A discontinuous-Galerkin finite element method for Darcy flow. *Computer Methods in Applied Mechanics and Engineering* 2006; **195**:3347–3381.
4. Brezzi F, Hughes TJR, Marini LD, Masud A. Mixed discontinuous Galerkin methods for Darcy flow. *SIAM Journal on Scientific Computing* 2005; **22**(1):119–145.
5. Bassi F, Rebay S. Discontinuous finite element high order accurate numerical solution of the compressible Navier–Stokes equations. In *Proceedings of the Conference Numerical Methods for Fluid Dynamics*, Morton KW *et al.* (eds), vol. V. Clarendon Press: Oxford, 3–6 April 1995; 295–302.
6. Baumann CE, Oden JT. A discontinuous *hp* finite element method for convection–diffusion problems. *Computer Methods in Applied Mechanics and Engineering* 1999; **175**:311–341.
7. Ayub M, Masud A. A new stabilized formulation for convective–diffusive heat transfer. *Numerical Heat Transfer, Part B* 2003; **44**:1–23.
8. Baiocchi C, Brezzi F, Franca LP. Virtual bubbles and Galerkin-least-squares type methods (Ga.L.S). *Computer Methods in Applied Mechanics and Engineering* 1993; **105**:125–141.
9. Brezzi F, Bristeau MO, Franca LP, Mallet M, Roge G. A relationship between stabilized finite element methods and the Galerkin method with bubble functions. *Computer Methods in Applied Mechanics and Engineering* 1992; **96**(1):117–129.
10. Brezzi F, Marini D, Russo A. Application of the pseudo residual-free bubbles to the stabilization of convection–diffusion problems. *Computer Methods in Applied Mechanics and Engineering* 1998; **166**:51–63.
11. Brezzi F, Franca LP, Hughes TJR, Russo A. $b = \int g$. *Computer Methods in Applied Mechanics and Engineering* 1997; **145**(3–4):329–339.



DOI: 10.1002/fld

12. Burman E, Hansbo P. Edge stabilization for Galerkin approximations of convection–diffusion problems. *Computer Methods in Applied Mechanics and Engineering* 2004; **193**(15–16):1437–1453.
13. Cockburn B, Dawson C. Approximation of the velocity by coupling discontinuous Galerkin and mixed finite element methods for flow problems. *Computational Geosciences* 2002; **6**:505–522.
14. Codina R, Soto O. Approximation of the incompressible Navier–Stokes equations using orthogonal-subscale stabilization and pressure segregation on anisotropic finite element meshes. *Computer Methods in Applied Mechanics and Engineering* 2004; **193**(15–16):1403–1419.
15. Coutinho ALGA, Dias CM, Alves JLD, Landau L, Loula AFD, Malta SMC, Castro RGS, Garcia ELM. Stabilized methods and post-processing techniques for Darcy flow and related problems. *Computer Methods in Applied Mechanics and Engineering* 2004; **193**(15–16):1421–1436.
16. Franca LP, Oliveira SP. Pressure bubbles stabilization features in the Stokes problem. *Computer Methods in Applied Mechanics and Engineering* 2003; **192**:1929–1937.
17. Franca LP, Nesliturk A. On a two-level finite element method for the incompressible Navier–Stokes equations. *International Journal for Numerical Methods in Engineering* 2001; **52**:433–453.
18. Masud A, Bergman LA. Application of multiscale finite element methods to the solution of the Fokker–Planck equation. *Computer Methods in Applied Mechanics and Engineering* 2005; **194**:1513–1526.
19. Masud A, Khurram R. A multiscale/stabilized finite element method for the advection–diffusion equation. *Computer Methods in Applied Mechanics and Engineering* 2004; **193**:1997–2018.
20. Masud A, Khurram R. A multiscale finite element method for the incompressible Navier–Stokes equations. *Computer Methods in Applied Mechanics and Engineering* 2006; **195**:1750–1777.
21. Khurram R, Masud A. A multiscale/stabilized formulation of the incompressible Navier–Stokes equations for moving boundary flows and fluid–structure interaction. *Computational Mechanics* 2006; **38**(4–5):403–416.
22. Nakshatrala KB, Turner D, Hjelmstad K, Masud A. A stabilized mixed finite element method for Darcy flow based on the multiscale decomposition of the solution. *Computer Methods in Applied Mechanics and Engineering* 2006; **195**:4036–4049.
23. Tezduyar TE. Computation of moving boundaries and interfaces and stabilization parameters. *International Journal for Numerical Methods in Fluids* 2003; **43**:555–575.
24. Tezduyar TE, Sathe S. Enhanced-discretization selective stabilization procedure (EDSSP). *Computational Mechanics* 2006; **38**:456–468.
25. Brezzi F, Fortin M. *Mixed and Hybrid Finite Element Methods*. Springer Series in Computational Mathematics, vol. 15. Springer: New York, 1991.
26. Raviart PA, Thomas JM. A mixed finite element method for second order elliptic problems. In *Mathematical Aspects of the Finite Element Method*, Galligani I, Magenes E (eds). Lecture Notes in Mathematics, vol. 606. Springer: New York, 1977.
27. Hughes TJR. Multiscale phenomena: Green's functions, the Dirichlet-to-Neumann formulation, subgrid scale models, bubbles and the origins of stabilized methods. *Computer Methods in Applied Mechanics and Engineering* 1995; **127**:387–401.
28. Hughes TJR, Franca LP. A new finite element formulation for computational fluid dynamics: VII. The Stokes problem with various well posed boundary conditions: symmetric formulations that converge for all velocity/pressure spaces. *Computer Methods in Applied Mechanics and Engineering* 1987; **65**:86–96.
29. Hughes TJR, Franca LP, Balestra M. A new finite element formulation for computational fluid dynamics: V. Circumventing the Babuska–Brezzi condition: a stable Petrov–Galerkin formulation of the Stokes problem accommodating equal-order interpolations. *Computer Methods in Applied Mechanics and Engineering* 1986; **59**:85–99.
30. Harari I, Hughes TJR. What are $C$ and $h$?: inequalities for the analysis and design of finite element methods. *Computer Methods in Applied Mechanics and Engineering* 1992; **97**:157–192.
31. Hughes TJR. *The Finite Element Method: Linear Static and Dynamic Finite Element Analysis*. Prentice-Hall: Englewoods Cliffs, NJ, 1987; Dover: New York, 2000.



DOI: 10.1002/fld